

https://dspace.org/

Polyvinyl AlcoholBased Cryogels Design Characterization and In Vitro Biological Studies

H Kula; S Motaung; M Razwinani; Samson Adeyemi; Philemon Ubanako ...

WILEY-BLACKWELL
https://hdl.handle.net/10539/48823
WOS

Downloaded from a DSpace repository. https://dspace.org/

Check for updates

Journal of Applied Polymer Science

WILEY

Applied Polymer SCIENCE

RESEARCH ARTICLE OPEN ACCESS

Polyvinyl Alcohol-Based Cryogels: Design, Characterization, and In Vitro Biological Studies

Hlalisa Kula[1] | Shirley Motaung[2] | Mapula Razwinani[2] | Samson A. Adeyemi[3] | Philemon Ubanako[3] | Lindokuhle M. Ngema[3] | T. Y. Fonkui[4] | D. T. Ndinteh[5] | Pradeep Kumar[3] | Yahya E. Choonara[3] | Blessing A. Aderibigbe[1]

[1]Department of Chemistry, University of Fort Hare, Alice, Eastern Cape, South Africa | [2]Global Health Biotech (PTY), Pretoria, South Africa | [3]Wits Advanced Drug Delivery Platform Research Unit, Department of Pharmacy and Pharmacology, School of Therapeutic Science, Faculty of Health Sciences, University of the Witwatersrand, Johannesburg, South Africa | [4]Department of Biotechnology and Food Technology, Faculty of Science, University of Johannesburg, Johannesburg, South Africa | [5]Drug Discovery and Smart Molecules Research Labs, Centre for Natural Product Research, Department of Chemical Sciences, University of Johannesburg, Johannesburg, South Africa

Correspondence: Blessing A. Aderibigbe (blessingaderibigbe@gmail.com)

Received: 24 December 2024 | **Revised:** 11 May 2025 | **Accepted:** 8 June 2025

Funding: This work was supported by the South African Medical Research Council (SAMRC) and THRIP.

Keywords: biocompatibility | biomaterials | biomedical applications | crosslinking | porous materials

ABSTRACT

Using inappropriate wound dressings makes the wound prone to bacteria invasion, impeding the wound-healing process. In this work, cryogels were prepared from selected polymers, such as polyvinyl alcohol (PVA), hydroxypropylmethylcellulose (HPMC), and sodium alginate (SA) via a freeze–thaw method and loaded with *Capparis sepiaria* plant extract to enhance the healing process. The cryogels displayed significant antibacterial activity against bacterial strains responsible for infected wounds. The prepared cryogels exhibited good tensile strength in the range of 0.06 ± 0.11–0.89 ± 0.66 MPa, moderate folding endurance between 1 ± 1.63 and 392 ± 17.18, and excellent porosity in the range of 76%–88.7% after 48 h. The water vapor transmission rate (WVTR) was in the range of 343 ± 18.67–3684 ± 16.70 g m^{-2}.day^{-1}. Remarkably, the cryogels displayed excellent biocompatibility with human cells, with cell viability of over 80%–100%. Furthermore, the wound-healing scratch assay yielded wound area coverage of > 60%, proving that the cryogels support cell adhesion and migration. The whole blood assay revealed the cryogels ability to prevent excessive bleeding. Results obtained from this work demonstrate the efficacy of plant extract-loaded cryogels as wound dressings for the treatment of microbial-infected and bleeding wounds.

1 | Introduction

The skin is prone to diseases and wounds because it protects the body from pathogens and also regulates blood and body temperature [1]. Microbes easily invade exposed wound areas and can result in damage to the underlying tissues surrounding the wound and prolong the healing process [2]. According to the duration in which they heal, wounds are classified as either acute (heal in a quick and orderly manner) or chronic (i.e., take much longer time to heal) [3]. Factors that deter the wound-healing process include underlying health conditions (obesity, diabetes, hypertension, etc.), old age, substance abuse, and the use of inappropriate wound dressings [4, 5]. It is imperative then to care for and manage all types of wounds using appropriate wound dressing materials to prevent them from not healing in good time. For a wound dressing to qualify as appropriate, it should keep that environment moist, be biodegradable and biocompatible, protect the wound from any bacterial invasion, prevent an accumulation of excessive exudates on the wound bed, support cell migration, and proliferation, and accelerate wound healing [6]. Wound dressing, such as cryogel offers the features of an ideal wound dressing.

This is an open access article under the terms of the Creative Commons Attribution-NonCommercial-NoDerivs License, which permits use and distribution in any medium, provided the original work is properly cited, the use is non-commercial and no modifications or adaptations are made.

© 2025 The Author(s). *Journal of Applied Polymer Science* published by Wiley Periodicals LLC.

Cryogels are hydrogels with an interconnected microporous structure. They are primarily prepared at very low temperatures by repeated freezing and thawing methods, resulting in the formation of interconnected pores [7]. These pores promote excellent exudate absorption, moisten the wound bed, contribute to the hemostatic property, and resist external distress [8]. Their porous structure resembles the extracellular matrix with good mechanical properties, making them promising wound dressings [8]. They can be prepared from bio- and synthetic polymers which include gum Arabic (GA), carboxymethylcellulose (CMC), sodium alginate (SA), hydroxypropylmethylcellulose (HPMC), and polyvinyl alcohol (PVA) [6]. SA has been widely utilized due to its biodegradable and biocompatible properties. It has antibacterial, anti-inflammatory, and antimicrobial properties [7]. SA has been used to develop cryogels with excellent hemostatic effects and is suitable for wounds with irregular edges [9, 10]. CMC is biodegradable and biocompatible with good solubility in water and has excellent swelling abilities [9]. CMC-based cryogels have been reported to display high swelling properties, significant antibacterial effects, and induce rapid hemostasis [11]. HPMC has transparent film-forming abilities. It is a good gelling agent useful to prepare wound dressings with controlled drug release, promotes a cooling/soothing effect on the wound, conforms well to irregular wound sizes, and is biocompatible for application to the skin [11]. GA is a viscosity-enhancing polymer used in wound dressing formulations, it is biocompatible and has been reported to possess anti-inflammatory and antioxidant properties [12]. PVA is water-soluble, biodegradable, and highly biocompatible. It can easily bind, thicken, and emulsify, and it is nontoxic and affordable [13]. It has been utilized to develop cryogel wound dressings with high swelling capability and high antimicrobial and antibiofilm formation properties that are useful for treating infected wounds [12, 13]. Apart from the use of polymers to develop wound dressings, the use of plant extracts in wound dressings needs to be explored.

Natural plant extracts have been explored by researchers due to the widely reported drug resistance that is common with most antibiotics [14]. This study delves into the development of polymer-based cryogels loaded with aqueous root extract of *Capparis sepiaria*, known for good antimicrobial and anti-inflammatory properties [15]. Incorporating the plant extract into the wound dressings provides a novel approach to accelerate the healing potential of the cryogels by bridging the gap between the widely reported antibiotic drug resistance and wound dressings that do not inhibit microbial invasion. In our recent finding, aqueous root extracts of *Capparis sepiaria* loaded into nanofibers displayed promising antibacterial activity suitable for treating infected wounds [16]. Other species of the Capparis plant, such as *Capparis zeylanica*, have been explored for the synthesis of titanium dioxide nanoparticles, which were administered topically on wounds, resulting in accelerated healing with significant antibacterial activity [17]. However, there is no report of cryogels loaded with *Capparis sepiaria* aqueous root extract for wound healing. The cryogel formulations were characterized using scanning electron microscopy (SEM), Fourier transform infrared spectroscopy (FTIR), water vapor transmission rate (WVTR), and pH, followed by evaluating their porosity, mechanical properties, and in vitro studies, including cytotoxicity, antibacterial, wound healing, and blood clotting assay.

2 | Materials and Methods

2.1 | Materials

The *Capparis sepiaria* plant extract was donated by Global Health Bio Tech (Pty) Ltd. South Africa. Polymers: SA, propylene glycol (PG), PVA, and gelatin (Gel) were purchased from Merck Chemicals South Africa. Reagents: sodium dihydrogen phosphate (NaH_2PO_4) and sodium hydroxide (NaOH) were also purchased from Merck Chemicals, South Africa. Other polymers, including carboxymethyl cellulose (CMC) and hydroxypropyl methylcellulose (HPMC), were bought from DB Fine Chemicals Specialities, South Africa. GA was purchased from Associated Chemical Enterprises, South Africa. Ethanol was acquired from Total Laboratory, South Africa, and glycerin from Clicks Pharmacy, South Africa. All the purchased chemicals did not require further purification, and distilled water was used to prepare the cryogels.

2.2 | *Capparis sepiaria* Plant Extract

The plant extract was evaluated using ultra-performance liquid chromatography-mass spectrometry (UPLC-MS), FTIR, and ultraviolet–visible spectroscopy (UV–vis). The results have been published by our research group [16].

2.3 | Preparation of Cryogels

The cryogels were prepared by a modified freeze–thaw method [18, 19]. The selected polymers shown in Table 1 were dissolved in distilled water and stirred with heating at 90°C for 2 h. Glycerine and propylene glycol were added dropwise to the polymer solution, followed by the addition of *Capparis sepiaria* plant extract. The resultant mixture was allowed to stir for a further 1 h. The polymer mixture was poured into a petri dish and left for 30 min before freezing at −20°C for 24 h and thawing at room temperature of 25°C. A total number of 6 cycles of freeze-thawing were performed until a soft spongy gel was obtained. The spongy gel was dried at room temperature and stored in a desiccator.

2.4 | Characterization

2.4.1 | Folding Endurance

The cryogels' folding endurance provides information on their flexibility and easy handling. It was performed by folding them manually and repeatedly at the same portion. It was performed in triplicates [20].

2.4.2 | Thickness of the Cryogels

The thickness of each cryogel was measured using a micrometer screw gauge. The measurement was performed at three selected portions of each cryogel, and the average of the three readings was reported for each dressing.

10974628, 2025, 39, Downloaded from https://onlinelibrary.wiley.com/doi/10.1002/app.57508 by University Of Witwatersrand, Wiley Online Library on [07/09/2025]. See the Terms and Conditions (https://onlinelibrary.wiley.com/terms-and-conditions) on Wiley Online Library for rules of use; OA articles are governed by the applicable Creative Commons License

TABLE 1 | The composition and combinations of the prepared cryogels.

Cryogel	PVA (g)	HPMC (g)	CMC (g)	SA (g)	GA (g)	Distilled water (mL)	Glycerine (mL)	Propylene glycol (mL)	Plant extract (g)
Blank	0.8	—		0.2	—	35	4	3	—
C1	1.0	—	1.0	—	—	76	4	3	0.2
C2	1.0	1.0	—	—	—	76	4	3	0.2
C3	1.0	—	—	3.0	—	100	4	3	0.2
C4	2.0	—	—	—	—	32	4	3	0.2
C5	—	2.0	—	—	—	60	4	3	0.2
C6	—	—	—	2.0	—	60	4	3	0.2
C7	1.0	—	—	—	1.0	36	4	3	0.2
C8	1.0	—	0.8	0.8	—	80	4	3	0.2

2.4.3 | Tensile Strength

The tensile strength of the five cryogels was performed on a Universal Tester (Instron universal testing machine, model 5966 (Instron, Norwood, MA, USA)), equipped with a 500 N load cell. D 882-18 Standard test method for tensile properties of thin sheeting was used to analyze the tensile strength of the cryogels. It was used to study the stiffness and flexibility of the cryogels. All samples were tested as received but after conditioning for 24 h at 20°C ± 2°C, and 65% ± 2% relative humidity. The samples were tested at a crosshead of 10 mm/min. The gauge length for each test was set at 30 mm. The measurements were done in triplicate. The tensile strength (TS) was determined using Equation (1).

$$\text{Tensile strength} = \frac{F}{X\,x\,Y} \tag{1}$$

where X is the width, Y is the thickness of the dressing, and F is the force applied to cause the cryogels to break [21].

2.4.4 | Water Vapor Transmission Rate (WVTR)

WVTR was calculated by mounting the dressings on a tube containing water and wrapped with Teflon tape. The weight changes over 24 h at 37°C were measured (Equation (2)) [22]. A number of three measurements were taken per sample for accuracy.

$$WVTR = \left(W_1 - W_2\right) \times 1000 \times 24 / T \tag{2}$$

where T is the test period in hours, W_1 is the initial cryogel weight, and W_2 is the final cryogel weight.

2.4.5 | pH Evaluation

To evaluate the pH of the wound dressings, they were placed in distilled water overnight at 25°C, and the pH was assessed using a pH meter (pH meter BASIC 20+ (Barcelona, Spain)) in triplicate to determine their suitability for dermal application [12].

2.4.6 | Porosity

The alcohol displacement method using anhydrous ethanol was explored to study the porosity of the cryogels. Each cryogel sample (10 mg) was placed in ethanol (1 mL) for 48 h, and the % porosity was determined using Equation (3) [23.24]. A number of three measurements were taken per sample for accuracy.

$$\%P = \frac{W_2 - W_1 - W_3}{W_2 - W_3} \times 100 \tag{3}$$

where W_1 is the initial mass of cryogel, W_2 is the mass of sample + ethanol, and W_3 is the final mass after time intervals.

2.4.7 | Fourier Transform Infrared Spectroscopy (FTIR)

FTIR analysis of the cryogels was performed using a Perkin Elmer Spectrum 100 spectrometer (Massachusetts, USA) in the range of 4000–400 cm^{-1}. The data obtained were analyzed using Origin Pro 2024 graphing and analysis software.

2.4.8 | Scanning Electron Microscopy (SEM)

The surface morphology of the cryogel dressings was viewed on JEOL JSM-6390 LV Scanning Electron Microscope (Tokyo, Japan). The cryogel samples were coated with gold nanoparticles, and the photomicrographs were captured at an accelerating voltage of 15 kV and a magnification of 1000×.

2.4.9 | X-Ray Diffraction (XRD)

XRD analysis was performed on a PAN analytical X'pert PRO (Eindhoven, Netherlands) equipped with a proportional counter using Cu–Kα ($\lambda = 0.154$ nm) radiation. Data were collected within the range of $2\theta = 5°–90°$, a voltage of 45 kV, and a current

10974628, 2025, 39, Downloaded from https://onlinelibrary.wiley.com/doi/10.1002/app.57508 by University Of Witwatersrand, Wiley Online Library on [07/09/2025]. See the Terms and Conditions (https://onlinelibrary.wiley.com/terms-and-conditions) on Wiley Online Library for rules of use; OA articles are governed by the applicable Creative Commons License

of 40 mA. The data were analyzed using Origin Pro 2024 graphing and analysis software.

2.4.10 | Biodegradation Studies

Biodegradation studies were performed under physiological conditions. 10 mg of each cryogel sample was placed in pH 5.5 and 7.4 buffer solutions (10 mL), simulating the pH of healthy skin and chronic wounds, respectively. The cryogel samples in buffer solutions were incubated in a Memmert Waterbath WNB 14 at 37°C for 3 weeks. The solutions were collected weekly (i.e., Weeks 1–3) and freeze-dried, followed by SEM and FTIR analysis [23].

2.4.11 | In Vitro Antibacterial Analysis

The efficacy of the eight cryogels against bacteria was evaluated through a known minimum inhibition concentration (MIC) method by Fonkui et al. [24]. Streptomycin, ampicillin, nalidixic acid, and *Capparis sepiaria* extract were all positive controls, and the negative control was 50% of nutrient broth in DMSO. Stock solutions were prepared by dissolving 4 mg of each cryogel in 5 mL of a mixture of DMSO and distilled H_2O (4:1, v/v). These solutions were then serially diluted (6 times) in 100 μL of nutrient broth in 96 well plates to the desired concentrations (400, 200, 100, 50, 25, and 12.5 μg/mL). Then, 100 μL of each of these solutions was placed in duplicate and seeded with 100 μL of an overnight bacterial culture brought to 0.5 McFarland in nutrient broth. The plates were incubated at 30°C for 24 h. Life or death cells were verified by the addition of resazurin dye (0.02%) to produce a pink color indicating the presence of viable cells and blue for dead cells. The minimum inhibitory concentrations of the controls streptomycin (STM) and nalidixic acid (NLD) against different bacterial strains and the bacterial strain's codes are included in Table 2.

2.4.12 | In Vitro Whole Blood Clot Assay

The in vitro whole blood clot assay was performed according to the protocol reported by Catanzano et al. [25] on selected cryogel formulations at a wavelength of 330 nm. Cryogel (2 mg) was added to whole blood (200 μL). The initiation of blood coagulation in the cryogel formulations was via the addition of $CaCl_2$ (20 μL). Incubation was performed for 10 min with gentle shaking at a temperature of 37°C, followed by the addition of deionized water (6 mL) to break down the red blood cells. The dilution of the blood samples to 25 mL was performed, and the relative absorbance was recorded on MS Excel.

2.4.13 | In Vitro Cytotoxicity Studies of the Cryogel Dressings

The in vitro cytotoxicity study was performed on selected cryogels with the highest efficacies in antibacterial studies to evaluate their nontoxicity using a known MTT assay against immortalized human keratinocytes (HaCaT cells) (Cellonex, Johannesburg, SA) [26]. The selected concentrations were 200, 100, 50, 25, 12.5, 6.25, and 3.125 μg/mL for 24 h. The HaCaT cells were cultured

TABLE 2 | The minimum inhibitory concentrations of the controls streptomycin (STM) and nalidixic acid (NLD) against different bacterial strains and the bacterial strains' codes.

Bacterial strain and code	Code name
Bacillus subtilis (ATCC19659)	BS
Enterococcus faecalis (ATCC13047)	EF
Mycobacterium smegmatis (MC2155)	MS
Staphylococcus epidermidis (ATCC14990)	SE
Escherichia coli (ATCC25922)	EC
Enterobacter cloacae (ATCC13047)	ECL
Klebsiella oxytoca (ATCC8724)	KO
Proteus vulgaris (ATCC6380)	PV
Pseudomonas aeruginosa (ATCC27853)	PA
Proteus mirabilis (ATCC7002)	PM
Staphylococcus aureus (ATCC25923)	SA
Klebsiella pneumonia (ATCC13882)	KP

in Dulbecco's Modified Eagle Medium (DMEM) supplemented with 10% fetal bovine serum (FBS) and 1% penicillin–streptomycin and incubated under humid conditions at 37°C and 5% CO_2. The cells were monitored until 90% confluence and thereafter seeded into 96-well plates at a density of 5×10^5 cells/mL for treatment. The positive control used is a commercially available wound dressing, BURN-EAZ, and the blank is cell-free wells. The cells were further incubated for 48 h for MTT analysis [26]. The absorbance readings were recorded at 570 nm using a Victor X3 multimodal microplate reader (PerkinElmer, Waltham, MA, USA). The % cell viability was then calculated using Equation (4).

$$\%\,\text{Cell viability} = \frac{\text{Absorbance sample compound} - \text{absorbance blank}}{\text{Absorbance untreated compound} - \text{absorbance blank}} \times 100 \quad (4)$$

2.4.14 | In Vitro Scratch Wound-Healing Assay

In vitro wound-healing assay was performed according to the procedure reported by Ranzato et al. [27] and Veeraperumal et al. [28]. HaCaT cells were cultured in a humidified incubator at 37°C and 5% CO_2 to 90% confluency in DMEM containing 10% FBS and 1% penicillin–streptomycin (Penstrep) antibiotics. The cells were then seeded (2.5×10^5 cells/mL) in 6-well plates for 48 h. Single scratch wounds per well were generated. The dislodged cells were removed by washing the cells with 2 mL of phosphate-buffered saline. Serum-poor DMEM (containing 1% FBS) was added (i.e., 1800 μL per well), and the cells treated with 200 μL of dressings were chosen from various concentrations that showed the highest viability on the MTT assay screen [29]. Cell migration and growth were monitored for over 72 h and quantified using ImageJ image processing software. The wound closure was calculated using the following Equation (5).

$$\% = \frac{\text{Wound area day 0} - \text{Wound closure day 4 (72 hr)}}{\text{Wound closure day 0}} \times 100 \quad (5)$$

10974628, 2025, 39, Downloaded from https://onlinelibrary.wiley.com/doi/10.1002/app.57508 by University Of Witwatersrand, Wiley Online Library on [07/09/2025]. See the Terms and Conditions (https://onlinelibrary.wiley.com/terms-and-conditions) on Wiley Online Library for rules of use; OA articles are governed by the applicable Creative Commons License

2.4.15 | Statistical Analysis

The results of the in vitro studies and others were evaluated using an unpaired students' *t*-test on GraphPad Prism version 9 (GraphPad Software Inc., San Diego, CA, USA) where the mean/average and standard deviation of the results were used to strengthen the validity of the findings. All the results obtained were expressed as mean ± SD, and $p \leq 0.05$ level was considered to be statistically significant.

3 | Results and Discussion

The UPLC-MS analysis of the *Capparis sepiaria* plant extract revealed several phytochemical constituents, namely gluconic acid, citric acid, epicatechin, and phloretin-2-o-glucoside, with molecular masses of 195.0500, 191.0208, 289.0389, and 435.1317, respectively [16]. These phytochemicals play a vital role in wound healing. Epicatechin, a flavonoid, is known for its potent antioxidant and anti-inflammatory effects, which help in balancing the wound environment and treating chronic wounds [30]. Gluconic acid, mostly known as gluconolactone, is one of the most common PHA acids (polyhydroxy acids) used in skincare and is commonly found in skin cells. It functions similarly to AHA (alpha hydroxy acid) and BHA (beta hydroxy acid), such as glycolic, lactic, and salicylic acids, by dissolving the "glue" that holds dead skin cells together [31]. Phloretin, another flavonoid, exhibits strong anti-inflammatory and antioxidant properties, along with antibacterial capabilities [32]. Citric acid has been found effective in treating chronic wound infections by reducing pH levels and inhibiting microbial growth on infected wounds [33].

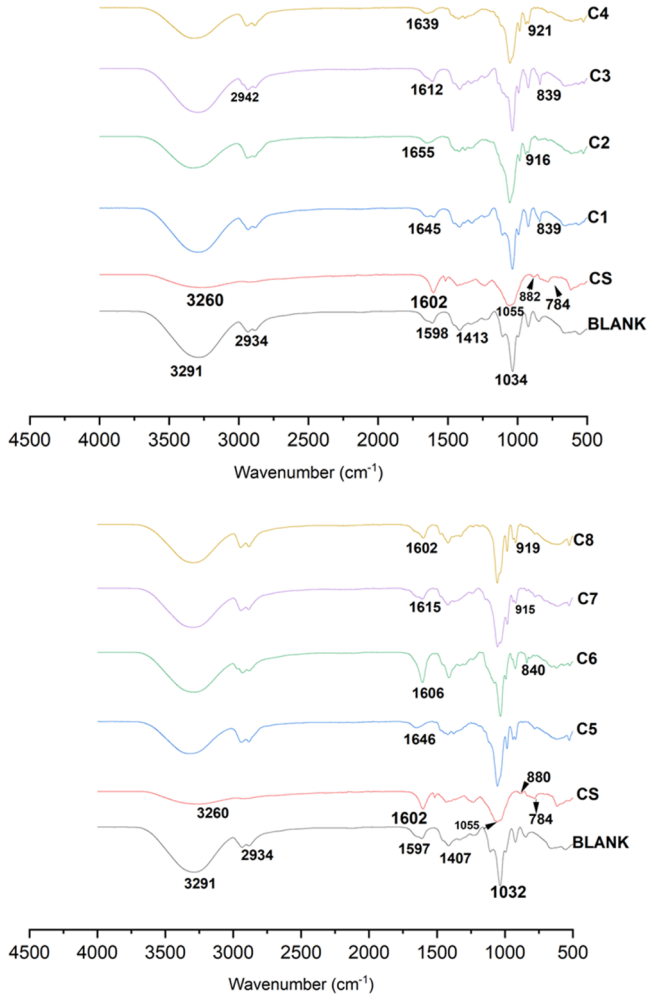

FIGURE 1 | FTIR spectra of plant extract, blank, and synthesized cryogel wound dressings, blank, C1–C4 and CS, C5–C8. [Color figure can be viewed at wileyonlinelibrary.com]

3.1 | Fourier Transform Infrared Spectroscopy (FTIR)

FTIR spectra of *Capparis sepieria* (CS) extract, blank, and cryogels are shown in Figure 1. The CS plant extract's FTIR spectra displayed peaks at 3260 cm^{-1} for a broad O—H stretch, at 1602–1516 cm^{-1} for C=C aromatic stretch, at 1430 cm^{-1} for alkanes C—H bend, sharp peak at 1233 for aryl ether C—O stretch from the phloretin-2-o-glucoside, 1055 cm^{-1} for C—O stretching of secondary alcohol, at 888 cm^{-1} for C—H bending of 1,2,4-trisubstituted, and at 786 cm^{-1} for C=C bending [16]. The FTIR spectrum of the blank cryogel showed characteristic peaks at 3291 cm^{-1} for O—H stretch, 2934 cm^{-1} and 2883 cm^{-1} for C—H stretch for aliphatic alkane, at 1610 cm^{-1} for C=O stretch, at 1413 cm^{-1} for —COO of SA, at 1030 cm^{-1} for C—O bend, at 993 cm^{-1} for C—O stretch due to carboxylate of SA and at 844 and 653 cm^{-1} for out-of-plane C—H bending and skeletal vibrations of PVA, respectively. The FTIR spectrum of the blank cryogel did not reveal a C=C aromatic alkene peak at 1600–1400 cm^{-1}, and the C=C bend around 786 cm^{-1}, showing the absence of the plant extract. The prepared cryogels, C1–C8, showed similar C=C prominent peaks of the plant extract, owing to the cyclic alkene in the phytochemical compounds present in the extract. C1 composed of PVA/CMC revealed significant peaks at 3388, 2936, 1415, 1041, and 1599 cm^{-1} for O—H stretch, C—H stretch, C—H bend, C—O stretch, and C=C stretch, respectively. C2 composed of PVA/HPMC showed absorption bands at 3329, 2942, 1650, 1421, and 1055 cm^{-1} for O—H, C—H, C=C stretch, C—H bending, and C—O stretch, respectively. C3 consisting of PVA/SA revealed significant peaks at 3296, 2936, 1611, 1415, and 1034 cm^{-1} for O—H, C—H, C=C, C—H bending, and C—O stretch. C4, C5, and C6 were prepared from a single polymer, that is, PVA, HPMC, or SA. C4 had significant peaks similar to pure PVA powder for the O—H, C—H, C—O, and C—H bend except for the peak at 1651 cm^{-1} for the C=C stretch owing to the plant extract. Similarly, C5 revealed peaks similar to pure HPMC powder for the O—H, C—H stretch, C—O, and C—H bend, except for the peak at 1651 cm^{-1} for the C=C stretch. C6, comprising of solely SA, had corresponding peaks at 3282 cm^{-1}, C—H stretch at 2929 cm^{-1}, 1042 cm^{-1} for —C—O stretching vibration, a weak peak for the carboxylate anion (—COO^{-}) from SA at 1323 cm^{-1}, 1606 cm^{-1} for C=C stretch, 1412 cm^{-1} for symmetric and asymmetric carbonyl —C=O. C7, comprising of PVA and GA, had significant absorption bands for O—H at 3282 cm^{-1}, two bands at 2949 cm^{-1} for C—H stretch, C=C stretching at 1606 cm^{-1}, 1041 cm^{-1} for C—O stretch, 1415 cm^{-1} and 1374 cm^{-1} for C—H bends. Cryogel C8 composed of PVA/CMC/SA showed prominent peaks, which were visible at 3296 cm^{-1} for a broad O—H stretch attributed to PVA, 2942 cm^{-1} for a C—H stretch, 1055 cm^{-1} for a C—O stretch, 1421 cm^{-1} for C—H bend, 1600 cm^{-1} for C=C stretch and 1326 cm^{-1} for the carboxylate anion of SA.

10974628, 2025, 39, Downloaded from https://onlinelibrary.wiley.com/doi/10.1002/app.57508 by University Of Witwatersrand, Wiley Online Library on [07/09/2025]. See the Terms and Conditions (https://onlinelibrary.wiley.com/terms-and-conditions) on Wiley Online Library for rules of use; OA articles are governed by the applicable Creative Commons License

The UPLC spectra revealed that the plant extract had four identified compounds present, with phloretin-2-o-glucoside being the most abundant, followed by epicatechin. The consistent peaks of 1599, 1650, 1611, 1651, 1651, 1606, 1606, 1600 cm^{-1} seen in C1, C2, C3, C4, C5, C6, C7, C8, respectively, attributed to the aromatic rings of phloretin-2-o-glucoside and epicatechin confirmed the successful loading of the plant extract into the cryogels. This also confirmed the successful crosslinking of the polymers PVA with either SA, CMC, GA, or HPMC for C1, C2, C3, C7, and C8. Moreover, upon comparison of the polymer's IR spectra, the sharp peak at 1600 cm^{-1} is not present, indicating that it is from the extract. The overall peaks in the IR spectra had shifts in the stretching modes, which could be attributed to hydrogen bonding, while the shifts in the bending mode could be due to alterations in molecular interactions (Figure S1) [34–37]. Similar peaks of similar combinations were reported by Bailik-Was et al. for SA/PVA-based hydrogels [38], PVA/CMC hydrogels by Shin et al. [39], Suksaeree et al. for PVA/HPMC patches [40], and Nasef et al. for PVA-GA nanocomposites [41]. The FTIR spectra of SA, CMC, GA, and HPMC are shown in Figure S2. No significant interaction was observed between the CS extract and the polymers. A similar finding was reported in our research group for hydrocolloids prepared from PVA and other polymers [42].

3.2 | Scanning Electron Microscopy

The SEM images of the cryogels, C1–C8, are shown in Figure 2. The morphology of most of the cryogels revealed by SEM analysis showed interwoven morphology for the cryogels, C1, C3, C5, and the blank. The presence of PVA played a significant role in the interwoven morphology. Similar findings have been reported for systems prepared from PVA [43–45]. Increasing the concentration of the formulation decreased the interwoven morphology significantly in cryogels C4 and C7. Similar findings were reported by Zhang et al. [43] for PVA-based films in which the interwoven fold lines were increasingly closer at increased PVA content. Cryogels were prepared from SA alone, and the combination of PVA with HPMC or with CMC and SA resulted in the absence of interwoven morphology in C2, C4, C6, C7, and C8. The interwoven morphology of the cryogels is similar to the ECM, with great potential to promote good gaseous uptake and cellular activities, such as cellular migration, proliferation, and essential features that promote skin regeneration [46]. ECM is composed of interwoven fibers that guide cellular growth and are characterized by high porosity and interconnected pores that maintain structural stability and provide optimal mechanical properties [46].

3.3 | X-Ray Diffraction (XRD)

The XRD spectra of the cryogels (Figure 3) demonstrate the amorphous nature of the cryogels and thus indicate that the CS plant extract was completely and uniformly dispersed within the cryogels' networks. The broad peaks of the XRD thermographs for the cryogels were visible with 2θ at 44.0°, 44.2°, 19.7°, 19.4°, 43.9°, 43.9°, 19.8°, and 20.3° for C1–C8, respectively. Sharp peaks with a higher intensity at 2θ values above 40.0° were visible in the XRD thermographs of cryogels C2 and C6, attributed to the plant extract. Similar findings were reported by Saranyaadevi et al. [47] for the XRD thermograph of green synthesized silver nanoparticles prepared using *Capparis zeylanica* plant extract with a significant 2θ at 43.47°.

3.4 | Mechanical Properties

The mechanical properties, such as thickness, folding endurance, and tensile strength, were performed on the cryogels (Table 3); stress–strain plots for each cryogel whose tensile strength was evaluated are included in the Supplementary Section (Figures S5–S8). The tensile strength of the cryogels ranged from 0.094 ± 0.03 to 12.261 ± 0.56 MPa. The cryogel with the highest tensile strength was C4, comprising only PVA, while the cryogel with the lowest tensile strength was C1, which consisted of a combination of PVA and CMC. The ideal tensile strength of wound dressings typically falls within the 1–32 MPa range and is considered suitable for skin application [48]. The tensile strength provides information on the strength, flexibility, and stability of the wound dressings when applied to the wound bed. Wounds on the joints or limbs require dressings with higher tensile strength, a feature that prevents the dressing from breaking [49]. The tensile strengths of the cryogels were considered to be suitable for the skin. The tensile strength of C1 was 0.094 MPa, which is similar to the findings reported by Li et al. [50] for PVA/CMC hydrogel, and they concluded that the low tensile strength may be attributed to a lack of strong hydrogen bonding between the polymers, resulting from inadequate freeze–thawing cycles. Hydrogen bonds are likely to form between all these formulations as hydroxyl groups are abundant in all the polymers and the compounds in the plant extract (Figure S1) [34–37]. However, the strength and distribution of these hydrogen bonds will vary due to the different polymers. If the hydrogen bonding is weaker or less effective in forming a cohesive network, it could lead to lower mechanical strength [50]. The effect of using glycerol was not studied; the same amount of glycerol was used for all the formulations. However, the analyzed cryogels revealed C4 and C5, prepared from only PVA and HPMC, displayed the highest tensile strengths compared to the blank cryogel and C6 prepared from SA only. Similar findings have been reported by Elgharbawy et al. [51] for films prepared from PVA alone that displayed high tensile strength when compared to films prepared from HPMC alone or used in combination with PVA and HPMC. In a report of films prepared from PVA by Yang et al. [52], the films prepared from SA alone displayed poorer tensile strength than the films prepared from PVA alone.

The thickness of the cryogels was in a range of 0.06 ± 0.11 to 0.89 ± 0.66 mm with a variation of 5 mm from the average, while the folding endurance was between 1 ± 1.63 and 392 ± 17.18. The thickness of the cryogels was influenced by the polymer concentration and the volume of the polymer solution poured into the petri dish, as reported by Pereira et al. [53]. Most of the cryogels displayed folding endurance values above 50%, indicating good flexibility. However, cryogels C1, C6, and C8 had relatively low folding endurance, which is attributed to the use of SA and PVA, which tends to yield brittle dressings [54]. Storing them in dry conditions can result in loss of moisture and further brittleness over time [53]. According to Wang et al. [55], the amount of

10974628, 2025, 39, Downloaded from https://onlinelibrary.wiley.com/doi/10.1002/app.57508 by University Of Witwatersrand, Wiley Online Library on [07/09/2025]. See the Terms and Conditions (https://onlinelibrary.wiley.com/terms-and-conditions) on Wiley Online Library for rules of use; OA articles are governed by the applicable Creative Commons License

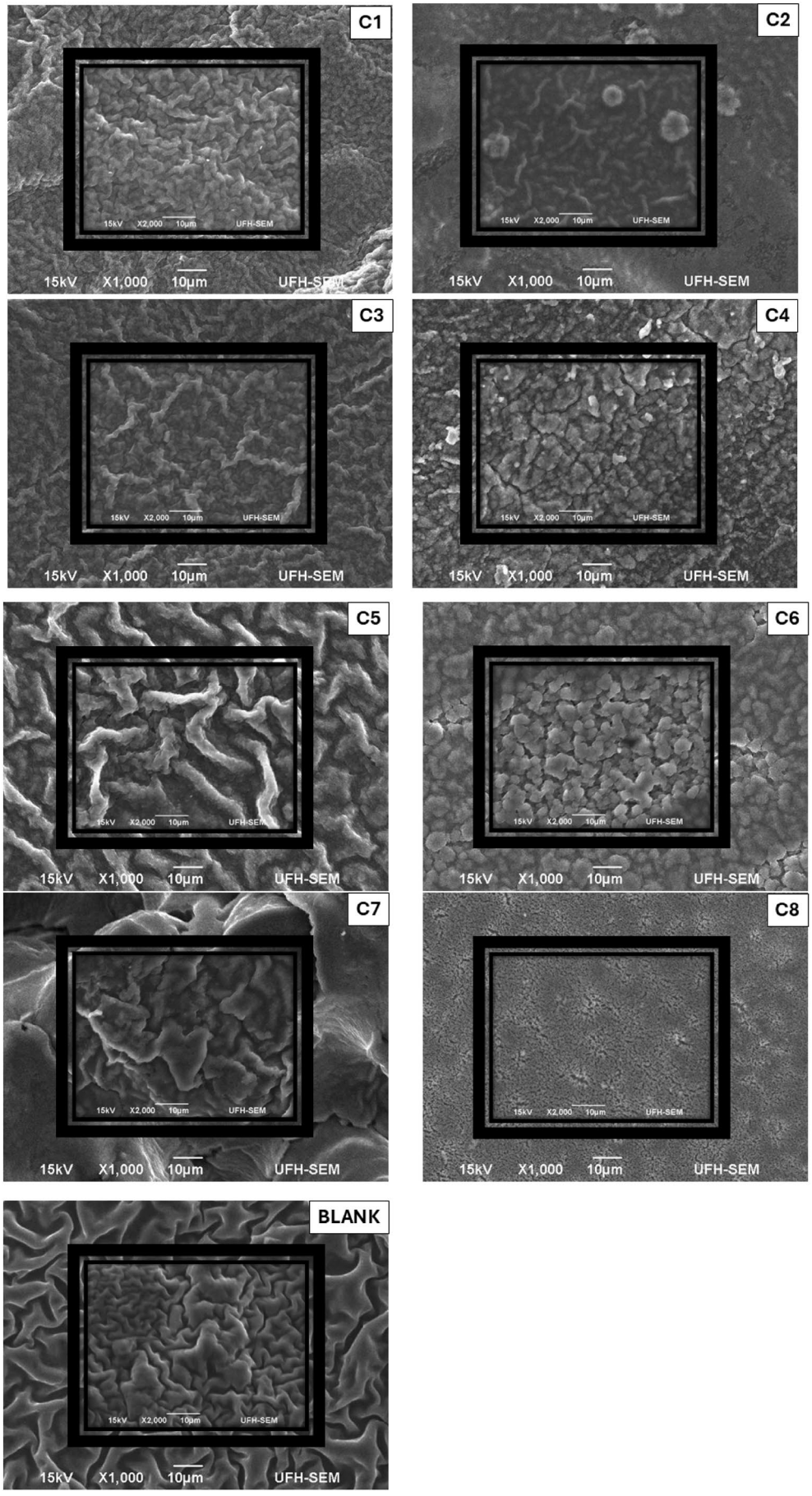

FIGURE 2 | SEM images of the prepared cryogels C1–C8 and blank.

10974628, 2025, 39, Downloaded from https://onlinelibrary.wiley.com/doi/10.1002/app.57508 by University Of Witwatersrand, Wiley Online Library on [07/09/2025]. See the Terms and Conditions (https://onlinelibrary.wiley.com/terms-and-conditions) on Wiley Online Library for rules of use; OA articles are governed by the applicable Creative Commons License

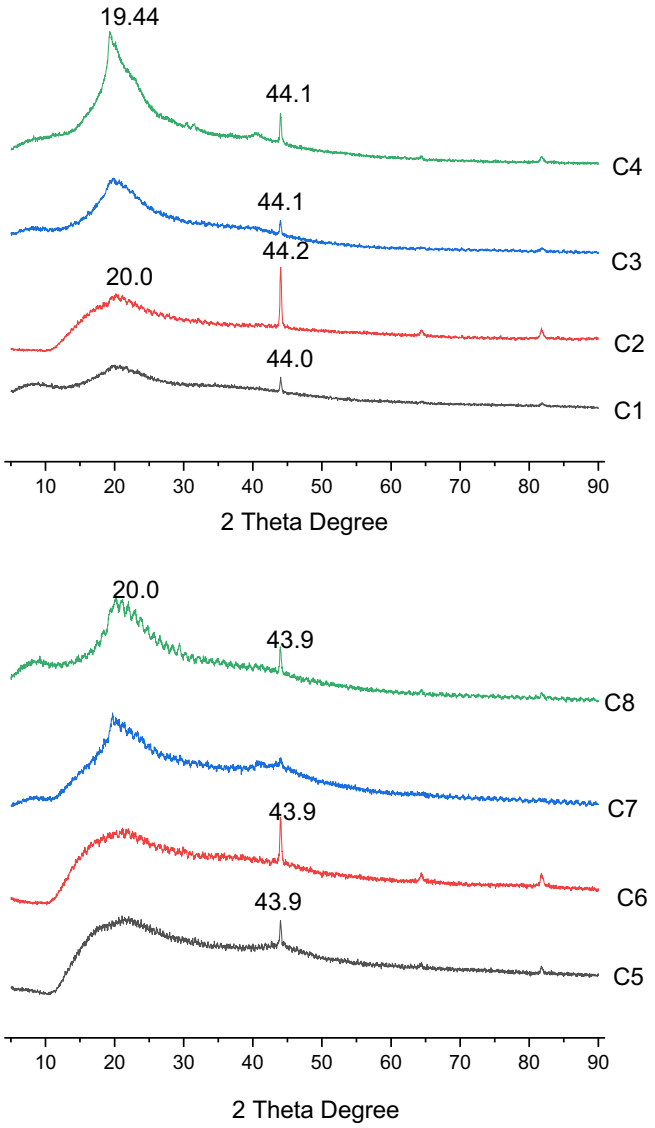

FIGURE 3 | XRD thermographs of C1–C4 and C5–C8. [Color figure can be viewed at wileyonlinelibrary.com]

TABLE 3 | Calculated mechanical properties of all the prepared cryogels.

Cryogel	Thickness (mean ± SD mm)	Tensile strength (MPa, mean ± SD)	Folding endurance
C1	0.76 ± 0.57	0.094 ± 0.03	1 ± 1.63
C2	0.14 ± 0.35	—	155 ± 24.02
C3	0.78 ± 0.54	4.657 ± 0.23	95 ± 9.92
C4	0.31 ± 0.39	12.261 ± 0.56	370 ± 56,49
C5	0.06 ± 0.11	8.878 ± 4.11	392 ± 17,18
C6	0.40 ± 0.09	2.884 ± 1.02	4 ± 1.63
C7	0.89 ± 0.66	—	85 ± 5.65
C8	0.65 ± 0.12	—	2 ± 1.63

glycerol used as a plasticizer results in the formation of hydrogen bonds due to glycerol containing multiple hydroxyl (—OH) groups that can form hydrogen bonds with the polymer chains. This interaction can compete with the hydrogen bonding between the polymer chains themselves, affecting the overall network structure. In some cases, glycerol can facilitate additional hydrogen bonding between the polymer and itself, potentially leading to a more complex network. This can improve the material's flexibility while still providing some level of strength [56]. It can be noted that properties such as folding endurance and thickness can be easily tailored by altering the composition and concentration of the polymer mixtures.

3.5 | Porosity, WVTR, and Surface pH of Cryogels

The porosity of biomaterials directly influences their performance [57]. The porosity of wound dressing has an effect on the fluid and gaseous exchange on the wound bed [58, 59]. The porosity of the cryogels ranged from 76% to 88.7% and was considered suitable for wound healing (Table 4). The porosity values were similar to those reported by Doozandeh et al. [60] for gelatin/GA-based wound dressings using the freeze-drying method. The freeze-thawing cycles influenced the overall porous nature of the dressings by creating a network of ice crystals within the gel structure during the freezing process [61]. When a gel is frozen, water molecules within the gel matrix form ice crystals, leading to the expansion of the gel and the formation of pores [61]. The cryogels are porous and will promote gas transmission and cell adhesion and proliferation in chronic wounds. Yokoyama et al. [62] reported highly elastic cryogels prepared from PVA with increased pore size, resulting from increased freezing–thawing cycles.

The free flow of oxygen to the wound site through the wound dressings is crucial for wound healing [63]. The cryogels displayed WVTR values in the range of 343 ± 18.67–3684 ± 16.70 g/m^2.day^{-1} (Table 4), which were similar to those reported by Simoes et al. [64]. The WVTR is influenced by properties such as thickness, porosity, and chemical properties of the materials used in their synthesis [65]. WVTR happens through the

TABLE 4 | Porosity, WVTR, and surface pH of prepared cryogels.

	Properties of cryogels		
Cryogel	Porosity after 48 h (% mean, SD)	WVTR (g/m^2.day^{-1})	pH
C1	79.5 ± 0.45	1951 ± 13.57	6.95 ± 0.35
C2	78.9 ± 0.30	3684 ± 16.70	6.68 ± 0.14
C3	80.8 ± 0.06	2328 ± 11.59	7.25 ± 1.44
C4	83.8 ± 0.02	1567 ± 44.88	6.40 ± 0.42
C5	75.8 ± 0.01	2664 ± 5.29	6.45 ± 0.14
C6	88.7 ± 0.22	3533 ± 9.14	6.39 ± 0.12
C7	77.9 ± 0.23	343 ± 18.67	6.18 ± 0.55
C8	76.0 ± 0.10	996 ± 6.68	6.8 ± 0.19

10974628, 2025, 39, Downloaded from https://onlinelibrary.wiley.com/doi/10.1002/app.57508 by University Of Witwatersrand, Wiley Online Library on [07/09/2025]. See the Terms and Conditions (https://onlinelibrary.wiley.com/terms-and-conditions) on Wiley Online Library for rules of use; OA articles are governed by the applicable Creative Commons License

hydrophilic sections of the cryogel and depends on the ratio of hydrophilicity to hydrophobicity of the components of the cryogels [65]. The reason for the increase in the WVTR is the increase in polymer contents, PVA, SA, HPMC, and plasticizers. CMC is said to be a hydrophilic polymer but tends to reduce the WVTR of dressings [65]. The wound dressings with WVTR values between 2000 and 2500 $g/m^2.day^{-1}$ are reported as the best for maintaining a moist environment at the wound site, as well as allowing water vapor exchanges [66]. Therefore, the WVTR values obtained for the cryogels make them better suited as wound dressings for dry and infected wounds.

The surface pH of the cryogels was measured. The cryogel dressings had pH values of 6.18–7.25, and most were within the pH range of normal skin (i.e., 4.0–6.8) [67]. According to Gethin [68], wound healing occurs most effectively at low pH, whereas alkaline wound environments have been linked predominately to chronic wounds, and thus the wound surface needs to be slightly acidic to promote cell proliferation and fibroblast formation and ultimately, the overall fast healing of the wound. The pH range of the prepared cryogels was observed to be appropriate for skin application. Commercially available wound dressings pH values have been reported to be between 5.25 and 7.90 [69]. Wounds disrupt the skin's natural acidic pH, exposing underlying tissue with a pH of 7.4 [70]. Most harmful bacteria that affect humans require pH levels above 6 to grow, but lower pH values inhibit their growth [71]. Therefore, wound dressings with an acidic pH are needed to hinder the growth of these bacteria, quickening the wound-healing process.

3.6 | Biodegradation Studies

The biodegradation studies of the cryogels were analyzed using FTIR (Figure S3) and SEM (Figure 4). The biodegradation studies were performed at pH 5.5 and 7.4 for C2, C4, and C5 for 3 weeks. Significant changes in the FTIR spectra and SEM images were observed after 3 weeks of the studies. The SEM and FTIR were analyzed by freeze–drying the cryogels after 3 weeks. The changes observed in the functional groups for the cryogels before and after degradation were determined using FTIR and are shown in the Supplementary Figures.

FTIR spectra of C2 and C4 after Week 3 at pH 7.4 and 5.5 showed that the peaks at 3272 (O—H), 2926 (C—H), 1647–1419 (=C—H), 1331 (COO), and 1067 (C—O) were visible. However, there was a decreased intensity of C—O stretch after biodegradation at pH of 7.4 and 5.5. The O—H peak intensity was increased at pH 7.4 but reduced at pH 5.5. The rate of degradation of C2 and C4 was not rapid. For C5, after biodegradation at pH 5.5, the C—H and O—H peaks were absent in the spectra, and the rest of the peaks at 1645, 1550, 1456, 1288, 1055, and 860 cm^{-1} were not significant. At pH 7.4, Week 3, most of the peaks disappeared, and the intensity of the O—H stretch reduced, leaving a peak at 1076 cm^{-1} and insignificant peaks between 2500 and 1198 cm^{-1}. The lack of significant peaks revealed the biodegradable nature of the cryogels. The rate of degradation of the wound dressings was gradual, thus indicating that they are structurally stable and capable of inducing skin regeneration [72]. Similar findings were reported by Bagri et al. [73] for PVA/Starch cryogels that showed the disappearance of significant peaks in the FTIR spectra.

The physical changes in the surface morphology of the cryogels before and after biodegradation are illustrated in Figure 4. All the cryogels showed a high level of surface roughness characterized by a fibrous and bead-shaped morphology, as observed in the SEM images compared to the images taken prior to the initiation of biodegradation studies. C2 and C5 surface morphologies changed from interwoven to irregular, while C4 had several pores after degradation. The pores of degraded cryogels became significant morphological evidence of degradation [73]. Moreover, the SEM images of degraded cryogels revealed disordered pores of the cryogel's surfaces due to the rupture of bonds in the network [73].

3.7 | In Vitro Antibacterial Studies

The MIC values of the cryogels and *Capparis sepiaria* plant extract are depicted in Table 5. MIC values were evaluated following the protocol reported by Fonkui et al. [24]. The cryogels displayed potent antibacterial effects against some bacterial strains with the blank that exhibited a MIC value of 15.625 μg/mL and was effective against *Enterococcus faecalis* when compared to STM (128 μg/mL), AMP (26 μg/mL), and NLD (512 μg/mL). The CS extract showed strong activity against some Gram-positive bacteria such as *Bacillus subtilis* (15.625 μg/mL), *Enterococcus faecalis* (15.625 μg/mL), *Staphylococcus aureus* (15.625 μg/mL), and *Enterobacter cloacae* (15.625 μg/mL) which show low MIC values, indicating that CS was very effective against these strains. The plant extract showed moderate activity against *Escherichia coli* (31.25 μg/mL), suggesting that CS may have some effectiveness against this Gram-negative bacterium but was less potent compared to the Gram-positive strains with low MIC values. It also showed limited effectiveness against other strains such as *Staphylococcus epidermidis* (500 μg/mL) and *Mycobacterium smegmatis* (500 μg/mL), indicating reduced effectiveness, suggesting that these strains are more resistant to the extract. *Klebsiella oxytoca* (500 μg/mL) and *Proteus mirabilis* (500 μg/mL) also show high MIC values, reflecting a similar resistance pattern. When compared with control antibiotics (AMP, STM, and NLD), CS demonstrates variable effectiveness and is particularly strong against certain Gram-positive strains. Saraswathi et al. [74] explored the antibacterial activities of an ethanol bark extract of *Capparis sepiaria* using the Agar Well diffusion method. Two strains, namely *Bacillus subtilis* (BS) and *Escherichia coli* (EC) had zones of inhibition of 15 and 14 mm for *Staphylococcus aureus* (SA) at 500 μg/mL concentrations [74]. All the strains CS was active against were the same ones the cryogels were potent against. The prominent trend observed among the prepared cryogels was the influence of PVA in the formulations. The cryogels with the highest levels of potency against the bacterial strains were all composed of PVA. C4, prepared from only PVA content, was the most potent of all cryogels, and C6, composed of only SA, did not display significant antibacterial efficacy. Similar findings were reported by Tamer et al. [75] for PVA/Kaolin composite sponges loaded with penicillin–streptomycin. The PVA film exhibited the greatest growth inhibition against all bacterial strains used in the study. While the antimicrobial effect of PVA may be limited, the addition of CS extract and other biopolymers, such as SA, GEL, and CMC, to the cryogel formulations could potentially enhance the antibacterial

10974628, 2025, 39, Downloaded from https://onlinelibrary.wiley.com/doi/10.1002/app.57508 by University Of Witwatersrand, Wiley Online Library on [07/09/2025]. See the Terms and Conditions (https://onlinelibrary.wiley.com/terms-and-conditions) on Wiley Online Library for rules of use; OA articles are governed by the applicable Creative Commons License

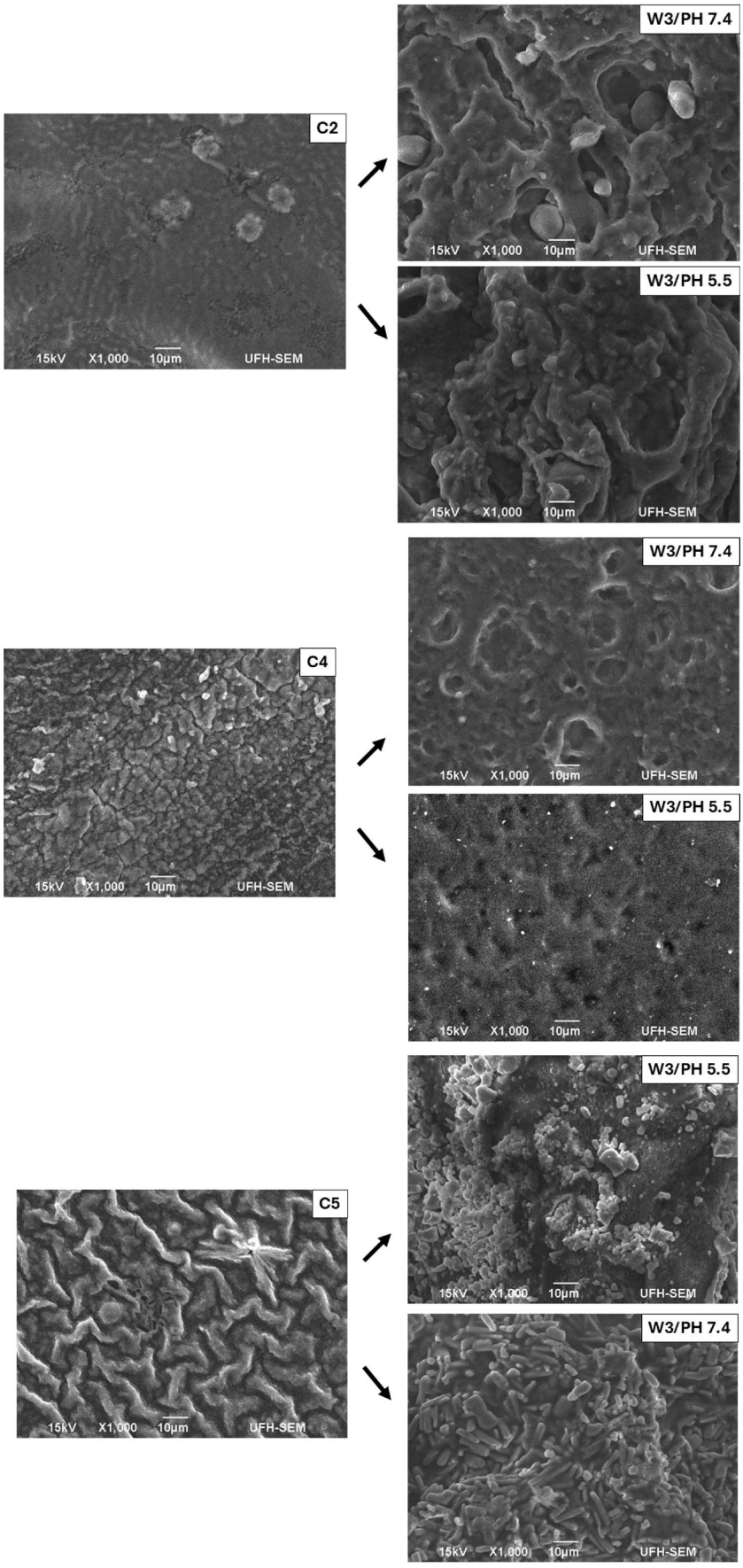

FIGURE 4 | SEM images for cryogels (C2, C4, and C5) before and after 3 weeks of biodegradation at pH 5.5 and 7.4.

10974628, 2025, 39, Downloaded from https://onlinelibrary.wiley.com/doi/10.1002/app.57508 by University Of Witwatersrand, Wiley Online Library on [07/09/2025]. See the Terms and Conditions (https://onlinelibrary.wiley.com/terms-and-conditions) on Wiley Online Library for rules of use; OA articles are governed by the applicable Creative Commons License

TABLE 5 | Minimum inhibitory concentration values of prepared cryogel dressings.

	Minimum inhibitory concentration (MIC, μg/mL)											
	Gram positive					Gram negative						
Cryogel	BS	EF	SE	SA	MS	ECL	PV	KO	PA	PM	EC	KA
BLANK	500	500	500	500	500	500	500	500	500	500	500	500
C1	500	500	500	500	15.625	15.625	500	500	500	500	500	500
C2	500	62.5	500	500	31.25	500	500	15.625	500	500	500	500
C3	500	31.25	500	500	500	31.25	15.625	15.625	15.625	500	500	500
C4	15.625	15.625	15.625	15.625	15.625	125	15.625	500	15.625	500	500	500
C5	500	500	15.625	500	500	500	500	31.25	500	31.25	500	15.625
C6	500	500	500	500	500	500	500	500	500	500	500	500
C7	500	15.625	500	500	500	15.625	15.625	15.625	15.625	15.625	15.625	500
C8	500	125	15.625	500	500	62.5	500	31.25	500	31.25	15.625	500
CS	15.625	15.625	500	15.625	500	15.625	15.625	500	15.625	500	31.25	500
AMP	26	26	26	26	26	26	416	26	64	26	26	26
STM	16	128	8	256	4	512	128	16	128	128	64	512
NLD	16	> 512	64	64	512	16	128	8	128	32	512	256

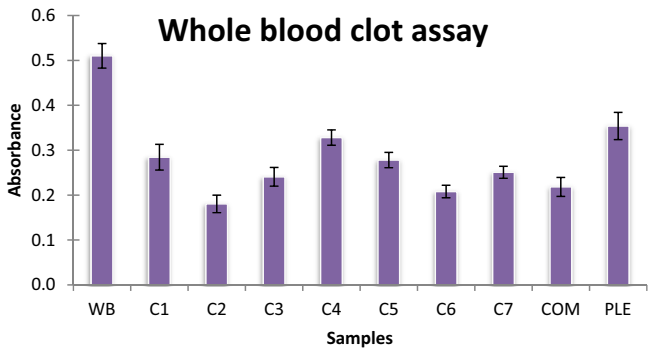

FIGURE 5 | Whole blood clot analysis (error bars ± STD) (where COM, commercial wound dressing (BURN-EAZ); PLE, *Capparis sepieria* extract, WB, whole blood). [Color figure can be viewed at wileyonlinelibrary.com]

activity, especially against resistant bacterial strains that cause infections. The presence of phytochemicals found in the aqueous extract of *Capparis sepiaria* contributes to its antibacterial activity [16]. The mechanism of action of phytochemicals on bacteria has been reported to be via the destruction of the bacterial membrane, the inhibition of the activity of enzymes and toxins, and the prevention of bacterial biofilm formation [76]. PVA-based materials and their combination with bioactive substances, such as plant extracts, result in potent antimicrobial efficacy and cell interactions to accelerate wound healing [77]. The prepared cryogels were active against common bacterial pathogens that are associated with chronic wound infections, including *Enterococcus faecalis, Staphylococcus aureus*, *Proteus vulgaris*, *Pseudomonas aeruginosa*, *Proteus mirabilis*, and *Enterobacter cloacae* [78]. These bacterial strains often develop antibiotic resistance and may multiply and invade traumatized skin, slowing down the rate of wound healing [78]. The formulated cryogels displayed good antibacterial efficacy, making them suitable for treating bacterial-infected wounds.

3.8 | In Vitro Whole Blood Clot Assay

The whole blood clot assay was performed to determine the hemostatic effect of the cryogels. Selected cryogels, C1–C7 were analyzed for hemostatic efficacy (Figure 5). The hemostatic effect of the selected cryogels was compared to the *Capparis sepiaria* plant extract and a commercial wound dressing, Burn-EAZ. The lower absorbance values tend to yield high blood clots [79]. Absorbance values of the cryogels (C1, C4, and C5) were lower when compared to the control ($p = 0.032$ for C1, 0.0022 for C4, and 0.0190 for C5). All the cryogels showed greater hemostatic efficacy than the plant extract ($p = 0.0448$ for C1, 0.0011 for C2, 0.0060 for C3, 0.0196 for C5, 0.0016 for C6, and 0.0058 for C7) except for C4 ($p = 0.2691$). Among the cryogel formulations, there was no significant difference in terms of the p value. The synthesized cryogels showed a more promising hemostatic effect than the plant extract, but only cryogels C2 and C6 showed a significant hemostatic effect than the commercial wound dressing. The reason for the absorbance trend of the cryogels is unclear and requires further studies. However, the presence of SA in the wound dressings played a crucial role in the absorbance values of C6, C3, and C7, resulting in lower absorbance values than the plant extract. Combining PVA with other polymers, such as SA, GA, CMC, and HPMC, also resulted in cryogels with promising hemostatic effects. Golafshan et al. [80] reported the good hemostatic properties of a PVA/SA nanohybrid hydrogel containing laponite, while Yang et al. [81] successfully developed PVA/CMC hydrogel and used PEG as a pore-forming agent using the freeze–thawing method to form macroporous dressings which enhanced the coagulation of blood. Ngece et al. [82] reported

10974628, 2025, 39, Downloaded from https://onlinelibrary.wiley.com/doi/10.1002/app.57508 by University Of Witwatersrand, Wiley Online Library on [07/09/2025]. See the Terms and Conditions (https://onlinelibrary.wiley.com/terms-and-conditions) on Wiley Online Library for rules of use; OA articles are governed by the applicable Creative Commons License

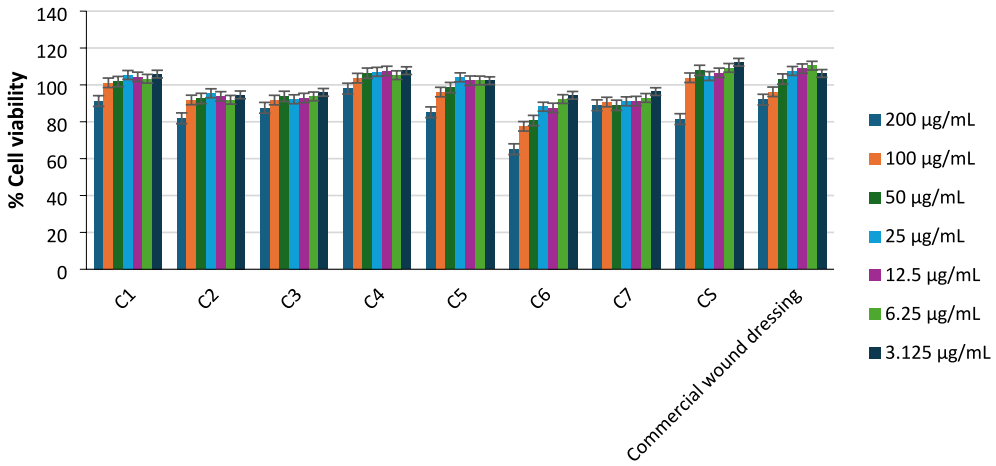

FIGURE 6 | %Cell viability versus concentration for C1–C7 against control (commercial wound dressing-BURN-EAZ) and plant extract, *C. sepiaria* (CS). [Color figure can be viewed at wileyonlinelibrary.com]

hemostatic Alginate/gum acacia sponges for bleeding wounds, and Yu et al. [83] also prepared hemostatic HPMC/Chitosan sponges. The results revealed that the polymers used contributed to the hemostatic effect of the cryogels.

3.9 | In Vitro Cytotoxicity

The in vitro cytotoxicity studies of the prepared cryogel dressings were evaluated in HaCaT cells using the MTT assay. The cryogels, C1–C7, a commercial wound dressing (Burn-EAZ), and the plant extract were selected for in vitro cytotoxicity at different concentrations (3.125, 6.25, 12.5, 25, 50, 100, and 200 µg/mL) over 96 h as indicated in Figure 6. The cryogels showed a high % cell viability of more than 90% at the concentrations of 3.125 and 25 µg/mL. The loading of *Capparis sepiaria* extract into the cryogels did not affect the cell viability ($p < 0.05$). All the cryogels exhibited high cell viability percentages, revealing their nontoxic and biocompatible nature [84]. There were no significant differences among the formulations themselves. This further proves the biocompatibility of the cryogels with the potential to support cell proliferation and migration, which is excellent for the overall management of infected wounds.

3.10 | In Vitro Scratch Wound-Healing Assay

In vitro wound-healing assay was done on selected prepared cryogels, C1, C4, and C5, at 0-, 24-, 48-, and 72-h time intervals to compare the rate of wound closure. The scratched cells were imaged to evaluate the cryogels' capability to support cell growth and proliferation (Figure 7). Treated cells showed a higher rate of closure compared to the untreated cells over the tested period of 72 h against HaCaT cells. The untreated cells had a low wound-healing reduction percentage of 20.63%, while C1, C4, and C5 were 60.39%, 62.99%, and 63.23%, respectively (Table 6). The control (BURN-EAZ), as expected, had a high reduction percentage of 71.43%. The commercial dressing, BURN-EAZ, was significantly different from C1, C4, and C5, with p values of 0.0433, 0.0347, and 0.0437, respectively. There were no significant differences between the formulations. The reduction brought about by the cryogels was moderate, with each formulation slightly above 60%. CMC, PVA, and HPMC are polymers that support cell growth and wound closure. Shin et al. [39] reported CMC/PVA hydrogels that supported cellular growth rapidly, as indicated by their scratch assay. Zanchetta et al. [85] reported HPMC/chitosan/insulin hydrogels that also supported cell migration. The cryogels are nontoxic to human cells and promote and stimulate cell proliferation.

4 | Conclusion

Chronic and infected wounds pose a great threat to humanity and reduce the life expectancy of humans as they have great potential to be fatal if left untreated properly. The cryogels were effectively prepared using the freeze-thawing method and incorporated well with the *Capparis sepiaria* plant extract. FTIR and XRD confirmed the physical stability and successful incorporation of the CS extract-loaded cryogels. SEM analysis revealed interwoven surface morphology, and the images were in agreement with the porosity evaluation, which was at a high range of 76%–88.7% after 48 h, indicating the cryogels' ability to absorb exudates and provide the wound with enough moisture to avoid desiccation. The pH was in the range of 6.18–7.25, which was considered suitable for infected wounds. It was also the same range as the currently used commercial wound dressings. The mechanical properties of the cryogels include tensile strength, which ranged between 0.346 ± 0.13 and 15.180 ± 4.86 MPa, thickness between 0.06 ± 0.11 and 0.89 ± 0.66 mm with a variation of 5 mm from the average while the folding endurance was between 1 ± 1.63 and 392 ± 17.18. Most cryogels were considered flexible and able to conform to several different types of wound sizes, and they were well adapted for skin application.

The WVTR of the prepared cryogels proved their capability to support gaseous exchange and their biodegradable nature. In vitro, antibacterial studies revealed the cryogels' potency combined with polymers used and the CS extract against Gram-positive and Gram-negative bacteria responsible for wound infections. The cryogel dressings were all found to be harmless to human cells as they showed a high % cell viability of more than 90% at the concentrations of 3.125 and 25 µg/mL. Additionally, they confirmed their ability to accelerate cell migration and

10974628, 2025, 39, Downloaded from https://onlinelibrary.wiley.com/doi/10.1002/app.57508 by University Of Witwatersrand, Wiley Online Library on [07/09/2025]. See the Terms and Conditions (https://onlinelibrary.wiley.com/terms-and-conditions) on Wiley Online Library for rules of use; OA articles are governed by the applicable Creative Commons License

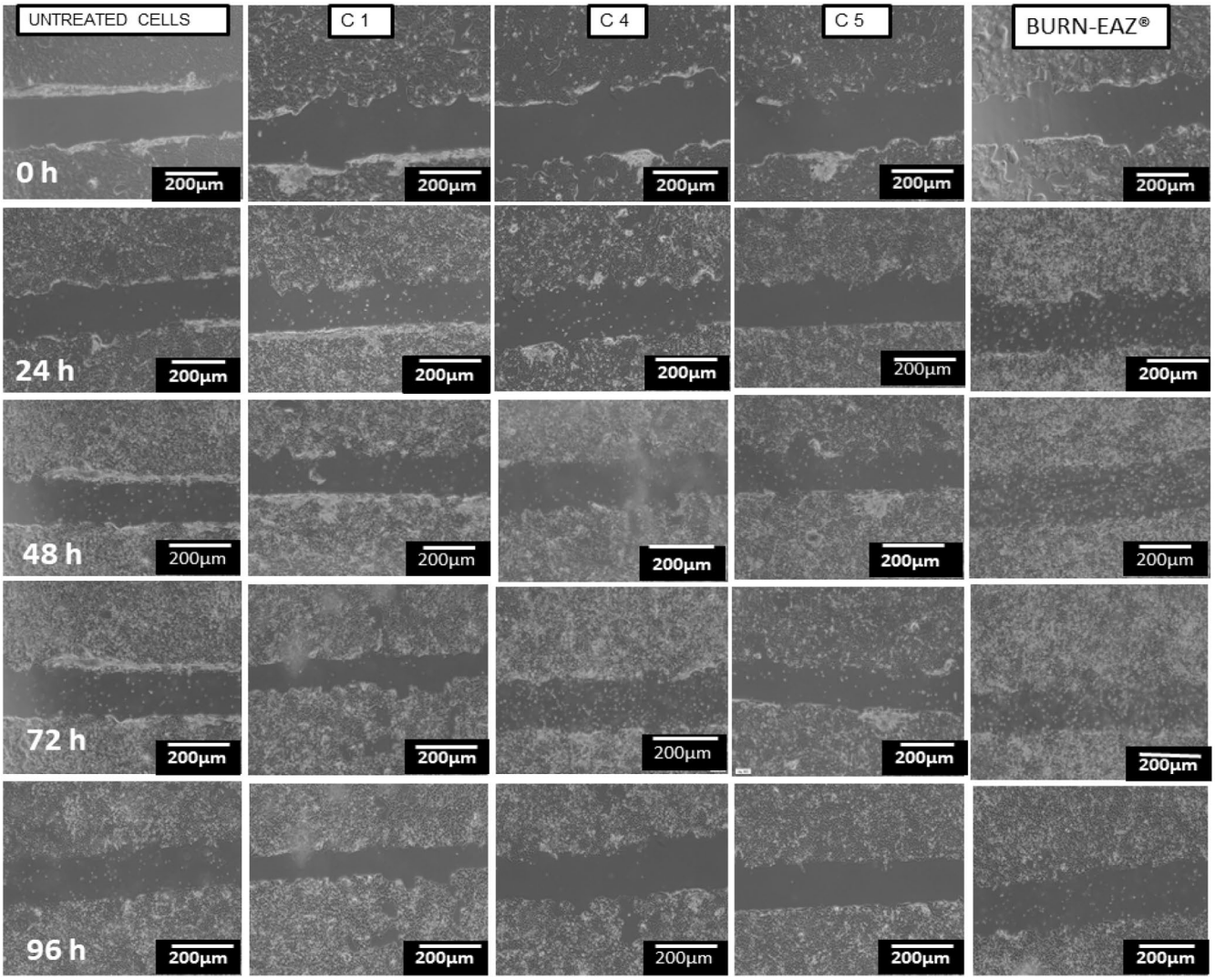

FIGURE 7 | Wound scratch healing of C1, C4, and C5 compared with untreated cells and the commercial dressing (BURN-EAZ) for 0, 24, 48, and 72.

TABLE 6 | Wound-healing reduction percentages for untreated cells, C1, C4, C5, and commercial dressing (Burn-Eaz) for 72 h.

Sample	Total wound reduction percentage
Untreated cells	19.36
C1	60.39
C4	62.99
C5	63.23
Control (BURN-EAZ)	71.43

growth, indicating their nontoxic and biocompatible nature and suitability for skin regeneration. The whole blood assay showed that all the cryogels showed greater hemostatic efficacy than the plant extract and are potentially suitable for bleeding wounds. The cryogels all displayed promising hemostasis, antibacterial, and wound-healing effects. However, further studies such as in vivo assay and transmission electron microscopy (TEM) are needed to visualize the microstructure of each cryogel and identify differences in pore size, shape, and distribution that can be directly linked to PVA presence and overall assess the full capabilities of the prepared cryogel dressings.

Author Contributions

Hlalisa Kula: data curation (lead), formal analysis (lead), investigation (lead), methodology (lead), validation (lead), writing – original draft (lead), writing – review and editing (lead). **Shirley Motaung:** conceptualization (lead), funding acquisition (lead), project administration (lead), resources (lead), supervision (lead). **Mapula Razwinani:** conceptualization (equal), data curation (equal), project administration (equal), resources (equal), validation (equal), visualization (equal). **Samson A. Adeyemi:** data curation (equal), formal analysis (equal), investigation (equal), methodology (equal), resources (equal), software (equal), validation (equal), visualization (equal), writing – review and editing (equal). **Philemon Ubanako:** data curation (equal), formal analysis (equal), investigation (equal), methodology (equal), project administration (equal), resources (equal), validation (equal), visualization (equal), writing – review and editing (equal). **Lindokuhle M. Ngema:** data curation (equal), formal analysis (equal), investigation (equal), methodology (equal), software (equal), validation (equal), visualization (equal), writing – review and editing (equal). **T. Y. Fonkui:** data

10974628, 2025, 39, Downloaded from https://onlinelibrary.wiley.com/doi/10.1002/app.57508 by University Of Witwatersrand, Wiley Online Library on [07/09/2025]. See the Terms and Conditions (https://onlinelibrary.wiley.com/terms-and-conditions) on Wiley Online Library for rules of use; OA articles are governed by the applicable Creative Commons License

curation (lead), formal analysis (lead), investigation (lead), methodology (equal), resources (equal), validation (equal), visualization (equal). **D. T. Ndinteh:** conceptualization (lead), investigation (lead), project administration (lead), resources (lead), visualization (lead). **Pradeep Kumar:** conceptualization (lead), data curation (lead), funding acquisition (lead), project administration (lead), resources (lead), software (lead), writing – review and editing (lead). **Yahya E. Choonara:** conceptualization (lead), data curation (lead), funding acquisition (lead), methodology (lead), project administration (lead), resources (lead), software (lead), validation (lead), writing – review and editing (lead). **Blessing A. Aderibigbe:** conceptualization (lead), formal analysis (lead), project administration (lead), resources (lead), supervision (lead), visualization (lead), writing – review and editing (lead).

Acknowledgments

The financial support of the National Research Foundation, Global Health Biotech (Pty) Ltd, University of Fort Hare, and Govan Mbeki Research and Development Centre for this research is hereby acknowledged.

Ethics Statement

The authors have nothing to report.

Conflicts of Interest

The authors declare no conflicts of interest.

Data Availability Statement

The data that support the findings of this study are available from the corresponding author upon reasonable request.

References

1. M. Ben Amar and M. Wu, "Re-Epithelialization: Advancing Epithelium Frontier During Wound Healing," *Journal of the Royal Society Interface* 11 (2014): 20131038.

2. J. D. Whitney, "Overview: Acute and Chronic Wounds," *Nursing Clinics* 40 (2005): 191–205.

3. S. A. Guo and L. A. DiPietro, "Factors Affecting Wound Healing," *Journal of Dental Research* 89 (2010): 219–229.

4. S. Kaya and S. Derman, "Properties of Ideal Wound Dressing," *Ankara Üniversitesi Eczacilik Fakültesi Dergisi* 47 (2023): 5.

5. B. A. Aderibigbe, "Hybrid-Based Wound Dressings: Combination of Synthetic and Biopolymers," *Polymers* 14 (2022): 3806.

6. N. K. Sachan, S. Pushkar, A. Jha, and A. J. Bhattcharya, "Sodium Alginate: The Wonder Polymer for Controlled Drug Delivery," *Journal of Pharmaceutical Research* 2 (2009): 1191–1199.

7. B. Akin and M. M. Ozmen, "Antimicrobial Cryogel Dressings Towards Effective Wound Healing," *Progress in Biomaterials* 11 (2022): 331–346.

8. L. Han, P. Li, P. Tang, et al., "Mussel-Inspired Cryogels for Promoting Wound Regeneration Through Photobiostimulation, Modulating Inflammatory Responses and Suppressing Bacterial Invasion," *Nanoscale* 11 (2019): 15846–15861.

9. P. Wu, R. H. He, Y. Fang, et al., "The Study of Double-Network Carboxymethyl Chitosan/Sodium Alginate Based Cryogels for Rapid Hemostasis in Noncompressible Hemorrhage," *International Journal of Biological Macromolecules* 266 (2024): 131399.

10. C. Liu, J. Liu, M. Wu, et al., "Cryogel Wound Dressings Based on Natural Polysaccharides Perfectly Adhere to Irregular Wounds for Rapid Haemostasis and Easy Disassembly," *Wound Repair and Regeneration* 32, no. 4 (2024): 393–406.

11. S. Cao, Q. Li, S. Zhang, Z. Liu, X. Lv, and J. Chen, "Preparation of Biodegradable Carboxymethyl Cellulose/Dopamine/ag NPs Cryogel for Rapid Hemostasis and Bacteria-Infected Wound Repair," *International Journal of Biological Macromolecules* 222 (2022): 272–284.

12. A. Górska, A. Krupa, D. Majda, et al., "Poly(Vinyl Alcohol) Cryogel Membranes Loaded With Resveratrol as Potential Active Wound Dressings," *AAPS PharmSciTech* 22 (2021): 1–15.

13. D. A. Elsherbiny, A. M. Abdelgawad, B. A. Hemdan, et al., "Self-Crosslinked Polyvinyl Alcohol/Cellulose Nanofibril Cryogels Loaded With Synthesized Aminophosphonates as Antimicrobial Wound Dressings," *Journal of Materials Chemistry B* 11 (2023): 7144–7159.

14. P. Rajesh, P. Selvamani, S. Latha, A. Saraswathy, and V. Kannan, "A Review on Chemical and Medicobiological Applications of Capparidaceae Family," *Pharmacognosy Reviews* 3 (2009): 378.

15. B. Singh, S. Sharma, and A. Dhiman, "Design of Antibiotic Containing Hydrogel Wound Dressings: Biomedical Properties and Histological Study of Wound Healing," *International Journal of Pharmaceutics* 457 (2013): 82–91.

16. S. P. Ndlovu, K. S. M. Motaung, S. A. Adeyemi, et al., "Sodium Alginate-Based Nanofibers Loaded With Capparis Sepiaria Plant Extract for Wound Healing," *Journal of Biomaterials Science, Polymer Edition* 22 (2024): 1–22.

17. M. Nilavukkarasi, S. Vijayakumar, M. Kalaskar, N. Gurav, S. Gurav, and P. K. Praseetha, "Capparis Zeylanica L. Conjugated TiO2 Nanoparticles as Bio-Enhancers for Antimicrobial and Chronic Wound Repair," *Biochemical and Biophysical Research Communications* 623 (2022): 127–132.

18. A. Chaturvedi, A. K. Bajpai, J. Bajpai, and S. K. Singh, "Evaluation of Poly (Vinyl Alcohol) Based Cryogel–Zinc Oxide Nanocomposites for Possible Applications as Wound Dressing Materials," *Materials Science & Engineering, C: Materials for Biological Applications* 65 (2016): 408–418.

19. P. Yu, C. Li, N. Zhu, S. N. Zhang, and G. J. Vancso, "Multifunctional and Recyclable Photothermally Responsive Cryogels as Efficient Platforms for Wound Healing," *Advanced Functional Materials* 29 (2019): 1904402.

20. J. C. Campos, D. Cunha, D. C. Ferreira, S. Reis, and P. J. Costa, "Oromucosal Precursors of In Loco Hydrogels for Wound-Dressing and Drug Delivery in Oral Mucositis: Retain, Resist, and Release," *Materials Science & Engineering, C: Materials for Biological Applications* 118 (2021): 111413.

21. H. Pan, D. Fan, W. Cao, et al., "Preparation and Characterization of Breathable Hemostatic Hydrogel Dressings and Determination of Their Effects on Full-Thickness Defects," *Polymers* 9 (2017): 727.

22. Y. Li, R. Fu, C. Zhu, and D. Fan, "An Antibacterial Bilayer Hydrogel Modified by Tannic Acid With Oxidation Resistance and Adhesiveness to Accelerate Wound Repair," *Colloids and Surfaces B: Biointerfaces* 205 (2021): 111869.

23. B. Buyana, B. A. Aderibigbe, S. S. Ray, D. T. Ndinteh, and Y. T. Fonkui, "Development, Characterization, and In Vitro Evaluation of Water Soluble Poloxamer/Pluronic-Mastic Gum-Gum Acacia-Based Wound Dressing," *Journal of Applied Polymer Science* 137, no. 21 (2019): 48728.

24. Y. T. Fonkui, M. I. Ikhile, P. B. Njobeh, and D. T. Ndinteh, "Benzimidazole Schiff Base Derivatives: Synthesis, Characterization and Antimicrobial Activity," *BMC Chemistry* 13 (2019): 1–11.

25. O. Catanzano, G. G. d'Ayala, A. D'Agostino, et al., "PEG-Crosslinked-Chitosan Hydrogel Films for In Situ Delivery of *Opuntia ficus*-Indica Extract," *Carbohydrate Polymers* 264 (2021): 117987.

26. M. Zare-Gachi, H. Daemi, J. Mohammadi, P. Baei, F. Bazgir, and S. Hosseini-Salekdeh, "Improving Anti-Hemolytic, Antibacterial and Wound Healing Properties of Alginate Fibrous Wound Dressings by Exchanging Counter-Cation for Infected Full-Thickness Skin Wounds,"

10974628, 2025, 39, Downloaded from https://onlinelibrary.wiley.com/doi/10.1002/app.57508 by University Of Witwatersrand, Wiley Online Library on [07/09/2025]. See the Terms and Conditions (https://onlinelibrary.wiley.com/terms-and-conditions) on Wiley Online Library for rules of use; OA articles are governed by the applicable Creative Commons License

Materials Science & Engineering, C: Materials for Biological Applications 107 (2020): 110321.

27. E. Ranzato, M. Patrone, L. Mazzucco, and B. Burlando, "Platelet Lysate Stimulates Wound Repair of HaCaT Keratinocytes," *British Journal of Dermatology* 159 (2008): 537–545.

28. S. Veeraperumal, H. M. Qiu, S. S. Zeng, et al., "Polysaccharides From Gracilaria Lemaneiformis Promote the HaCaT Keratinocytes Wound Healing by Polarised and Directional Cell Migration," *Carbohydrate Polymers* 241 (2020): 116310.

29. W. Strober, "Trypan Blue Exclusion Test of Cell Viability," *Current Protocols in Immunology* 111 (2015): A–3B.

30. K. Kantikosum, Y. Chongpison, N. Chottawornsak, and P. Asawanonda, "The Efficacy of Glycolic Acid, Salicylic Acid, Gluconolactone, and Licochalcone A Combined With 0.1% Adapalene vs Adapalene Monotherapy in Mild-To-Moderate *Acne vulgaris*: A Double-Blinded Within-Person Comparative Study," *Clinical, Cosmetic and Investigational Dermatology* 12 (2019): 151–161.

31. J. B. Johnson, D. A. Broszczak, J. S. Mani, J. Anesi, and M. Naiker, "A Cut Above the Rest: Oxidative Stress in Chronic Wounds and the Potential Role of Polyphenols as Therapeutics," *Journal of Pharmacy and Pharmacology* 74 (2022): 485–502.

32. R. Du, Q. Lv, W. Hu, et al., "Phloretin Potentiates Polymyxin E Activity Against Gram-Negative Bacteria," *Life Sciences* 287 (2021): 120085.

33. S. Tandon, B. Singh, S. Kapoor, and S. Mangal, "Comparison of Effect of pH Modulation on Wound Healing With Topical Application of Citric Acid Versus Superoxide Ions," *Nigerian Journal of Surgery* 26 (2020): 122–126.

34. Q. Zhou, S. Lu, C. Huang, et al., "Polyvinyl Alcohol/Sodium Alginate Hydrogels With Tunable Mechanical and Conductive Properties for Flexible Sensing Applications," *International Journal of Biological Macromolecules* 283 (2024): 137822.

35. K. Pratinthong, W. Punyodom, P. Jantrawut, et al., "Modification of a Carboxymethyl Cellulose/Poly(Vinyl Alcohol) Hydrogel Film With Citric Acid and Glutaraldehyde Crosslink Agents to Enhance the Anti-Inflammatory Effectiveness of Triamcinolone Acetonide in Wound Healing," *Polymers* 16 (2024): 1798.

36. A. Saeed, G. M. Asnag, A. M. Alghamdi, et al., "Structural, Optical, and Electrical Characteristics of HPMC/PVA-I2O5 Composites: Fabrication and Performance Analysis for Energy Storage Applications," *Journal of Energy Storage* 96 (2024): 112765.

37. W. Falath, A. Sabir, and K. I. Jacob, "Novel Reverse Osmosis Membranes Composed of Modified PVA/Gum Arabic Conjugates: Biofouling Mitigation and Chlorine Resistance Enhancement," *Carbohydrate Polymers* 155 (2017): 28–39.

38. K. Bialik-Wąs, K. Pluta, D. Malina, M. Barczewski, K. Malarz, and A. Mrozek-Wilczkiewicz, "Advanced SA/PVA-Based Hydrogel Matrices With Prolonged Release of Aloe Vera as Promising Wound Dressings," *Materials Science and Engineering: C* 120 (2021): 111667.

39. J. Y. Shin, D. Y. Lee, J. I. Yoon, and Y. S. Song, "Effect of CMC Concentration on Cell Growth Behavior of PVA/CMC Hydrogel," *Macromolecular Research* 28 (2020): 813–819.

40. J. Suksaeree, N. Nawathong, R. Anakkawee, and W. Pichayakorn, "Formulation of Polyherbal Patches Based on Polyvinyl Alcohol and Hydroxypropylmethyl Cellulose: Characterization and In Vitro Evaluation," *AAPS PharmSciTech* 18 (2017): 2427–2436.

41. S. Nasef, E. ElNesr, F. Hafez, N. Badawy, and S. Slim, "Gamma Irradiation Induced Preparation of Gum Arabic/ Poly (Vinyl Alcohol) Copolymer Hydrogels for Removal of Heavy Metal Ions From Wastewater," *Arab Journal of Nuclear Sciences and Applications* 53 (2020): 208–221.

42. H. Kula, S. Motaung, S. A. Adeyemi, et al., "Development and In Vitro Biological Evaluation of Hydrocolloid-Based Wound Dressings Incorporated WithCapparis sepiariaExtract," *Journal of Applied Polymer Science* 142 (2025): e56809.

43. H. Zhang, M. Li, Z. Liu, and Y. Cao, "Heat-Sealable, Transparent, and Degradable Arabinogalactan/Polyvinyl Alcohol Films With UV-Shielding, Antibacterial, and Antioxidant Properties," *International Journal of Biological Macromolecules* 275 (2024): 133535.

44. Z. Ren, F. Guo, Y. Wen, Y. Yang, J. Liu, and S. Cheng, "Strong and Anti-Swelling Nanofibrous Hydrogel Composites Inspired by Biological Tissue for Amphibious Motion Sensors," *Materials Horizons* 22 (2024): 5600–5613.

45. D. Kaur and A. Kaur, "Engineering of Electrospun Polycaprolactone/Polyvinyl Alcohol-Collagen Based 3D Nano Scaffolds and Their Drug Release Kinetics Using Cetirizine as a Model Drug," *International Journal of Biological Macromolecules* 268 (2024): 131847.

46. P. Y. Feng and X. Jing, "Novel Shish-Kebab Structured Nanofibrous Decorating Chitosan Unidirectional Scaffolds to Mimic Extracellular Matrix for Tissue Engineering," *Journal of the Mechanical Behavior of Biomedical Materials* 158 (2024): 106677.

47. K. Saranyaadevi, V. Subha, R. E. Ravindran, and S. A. Renganathan, "Green Synthesis and Characterization of Silver Nanoparticle Using Leaf Extract of *Capparis zeylanica*," *Asian Journal of Pharmaceutical and Clinical Research* 7 (2014): 44–48.

48. N. A. Annaidh, K. Bruyère, M. Destrade, and M. D. Gilchrist, "Characterization of the Anisotropic Mechanical Properties of Excised Human Skin," *Journal of the Mechanical Behavior of Biomedical Materials* 5 (2012): 139–148.

49. S. Thomas, G. Hughes, P. Fram, and A. Hallett, "An In-Vitro Comparison of the Physical Characteristics of Hydrocolloids, Hydrogels, Foams and Alginate/CMC Fibrous Dressings," *SMTL* 1 (2005): 1–24.

50. Y. Li, C. Zhu, D. Fan, et al., "Construction of Porous Sponge-Like PVA-CMC-PEG Hydrogels With pH-Sensitivity via Phase Separation for Wound Dressing," *International Journal of Polymeric Materials and Polymeric Biomaterials* 69 (2020): 505–515.

51. A. S. Elgharbawy, A. G. El Demerdash, W. A. Sadik, M. A. Kasaby, A. H. Lotfy, and A. I. Osman, "Synthetic Degradable Polyvinyl Alcohol Polymer and its Blends With Starch and Cellulose—A Comprehensive Overview," *Polymer* 16, no. 10 (2024): 1356.

52. M. Yang, J. Shi, and Y. Xia, "Effect of SiO_2, PVA and Glycerol Concentrations on Chemical and Mechanical Properties of Alginate-Based Films," *International Journal of Biological Macromolecules* 107 (2018): 2686–94.

53. R. Pereira, A. Carvalho, D. C. Vaz, M. H. Gil, A. Mendes, and P. Bártolo, "Development of Novel Alginate Based Hydrogel Films for Wound Healing Applications," *International Journal of Biological Macromolecules* 52 (2013): 221–230.

54. V. Cyriac, K. Mishra, Y. N. Sudhakar, Z. E. Rojudi, S. P. Masti, and I. M. Noor, "Suitability of NaI Complexed Sodium Alginate-Polyvinyl Alcohol Biodegradable Polymer Blend Electrolytes for Electrochemical Device Applications: Insights Into Dielectric Relaxations and Scaling Studies," *Solid State Ionics* 411 (2024): 116578.

55. X. Wang, H. Zhang, X. Zhang, et al., "A Comparison Study on Effects of Polyglycerols on Physical Properties of Alginate Films," *International Journal of Biological Macromolecules* 254 (2024): 127879.

56. R. Ma, Y. Wang, H. Qi, et al., "Nanocomposite Sponges of Sodium Alginate/Graphene Oxide/Polyvinyl Alcohol as Potential Wound Dressing: In Vitro and In Vivo Evaluation," *Composites Part B: Engineering* 167 (2019): 396–405.

57. P. S. Kumar, G. Praveen, M. Raj, K. P. Chennazhi, and R. Jayakumar, "Flexible, Micro-Porous Chitosan–Gelatin Hydrogel/Nanofibrin Composite Bandages for Treating Burn Wounds," *RSC Advances* 4 (2014): 65081–65087.

10974628, 2025, 39, Downloaded from https://onlinelibrary.wiley.com/doi/10.1002/app.57508 by University Of Witwatersrand, Wiley Online Library on [07/09/2025]. See the Terms and Conditions (https://onlinelibrary.wiley.com/terms-and-conditions) on Wiley Online Library for rules of use; OA articles are governed by the applicable Creative Commons License

58. O. Akiyode and J. Boateng, "Composite Biopolymer-Based Wafer Dressings Loaded With Microbial Biosurfactants for Potential Application in Chronic Wounds," *Polymers* 10 (2018): 918.

59. M. C. Koetting, J. T. Peters, S. D. Steichen, and N. A. Peppas, "Stimulus-Responsive Hydrogels: Theory, Modern Advances, and Applications," *Materials Science & Engineering R: Reports* 93 (2015): 1–49.

60. Z. Doozandeh, S. Saber-Samandari, and A. Khandan, "Preparation of Novel Arabic Gum–C_6H_9NO Biopolymer as a Bedsore for Wound Care Application," *Acta Medica Iranica* 58 (2020): 520–530.

61. H. Zhang, C. Liu, L. Chen, and B. Dai, "Control of Ice Crystal Growth and Its Effect on Porous Structure of Chitosan Cryogels," *Chemical Engineering Science* 201 (2019): 50–57.

62. F. Yokoyama, I. Masada, K. Shimamura, T. Ikawa, and K. Monobe, "Morphology and Structure of Highly Elastic Poly(Vinyl Alcohol) Hydrogel Prepared by Repeated Freezing-And-Melting," *Colloid and Polymer Science* 264 (1986): 595–601.

63. P. Wu, A. C. Fisher, P. P. Foo, D. Queen, and J. D. Gaylor, "In Vitro Assessment of Water Vapour Transmission of Synthetic Wound Dressings," *Biomaterials* 16 (1995): 171–175.

64. D. Simões, *PhD Diss* (Universidade da Beira Interior (Portugal), 2018).

65. S. Mahmood, N. R. Khan, G. Razaque, et al., "Microwave-Treated Physically Cross-Linked Sodium Alginate and Sodium Carboxymethyl Cellulose Blend Polymer Film for Open Incision Wound Healing in Diabetic Animals—A Novel Perspective for Skin Tissue Regeneration Application," *Pharmaceutics* 15 (2023): 418.

66. T. Khaliq, M. Sohail, M. U. Minhas, et al., "Self-Crosslinked Chitosan/κ-Carrageenan-Based Biomimetic Membranes to Combat Diabetic Burn Wound Infections," *International Journal of Biological Macromolecules* 197 (2022): 157–168.

67. M. Hildegrad, S. Wendtner, and H. C. Korting, *pH and Skin Care* (ABW Wissenschaftsverlag GmbH, 2007), 22–23.

68. G. Gethin, "The Significance of Surface pH in Chronic Wounds," *Wounds UK* 3 (2007): 52–56.

69. S. L. Percival, S. McCarty, J. A. Hunt, and E. J. Woods, "The Effects of pH on Wound Healing, Biofilms, and Antimicrobial Efficacy," *Wound Repair and Regeneration* 22 (2014): 174–186.

70. M. U. Uzun, S. C. Anand, and T. Shah, "The Effect of Wound Dressings on the pH Stability of Fuids," *Journal of Wound Care* 21 (2012): 88–95.

71. H. C. Korting, *Skin Cleansing With Synthetic Detergents: Chemical, Ecological, and Clinical Aspects* (Springer Berlin Heidelberg, 1992), 87–96.

72. Z. Mbese, S. Alven, and B. A. Aderibigbe, "Collagen-Based Nanofibers for Skin Regeneration and Wound Dressing Applications," *Polymers* 13 (2021): 4368.

73. L. P. Bagri, J. Bajpai, and A. K. Bajpai, "Evaluation of Starch Based Cryogels as Potential Biomaterials for Controlled Release of Antibiotic Drugs," *Bulletin of Materials Science* 34 (2011): 1739–1748.

74. K. Saraswathi, C. Sivaraj, A. Jenifer, M. Dhivya, and P. Arumugam, "Antioxidant, Antibacterial Activities, GCMS and FTIR Analysis of Ethanol Bark Extract of Capparis Sepiaria L.," *Research Journal of Pharmacy and Technology* 13 (2020): 2144–2150.

75. T. M. Tamer, M. M. Sabet, A. M. Omer, et al., "Hemostatic and Antibacterial PVA/Kaolin Composite Sponges Loaded With Penicillin–Streptomycin for Wound Dressing Applications," *Scientific Reports* 11 (2021): 3428.

76. R. Barbieri, E. Coppo, A. Marchese, et al., "Phytochemicals for Human Disease: An Update on Plant-Derived Compounds Antibacterial Activity," *Microbiological Research* 196 (2017): 44–68.

77. M. Teodorescu, M. Bercea, and S. Morariu, "Biomaterials of PVA and PVP in Medical and Pharmaceutical Applications: Perspectives and Challenges," *Biotechnology Advances* 37 (2019): 109–131.

78. H. Guan, W. Dong, Y. Lu, et al., "Distribution and Antibiotic Resistance Patterns of Pathogenic Bacteria in Patients With Chronic Cutaneous Wounds in China," *Frontiers in Medicine* 8 (2021): 609584.

79. X. Huang, Q. Fu, Y. Deng, et al., "Surface Roughness of Silk Fibroin/Alginate Microspheres for Rapid Hemostasis in Vitro and In Vivo. Carbohydrate Polymers," *Carbohydrate Polymers* 253 (2021): 117256.

80. N. Golafshan, R. Rezahasani, M. T. Esfahani, M. Kharaziha, and S. N. Khorasani, "Nanohybrid Hydrogels of Laponite: PVA-Alginate as a Potential Wound Healing Material," *Carbohydrate Polymers* 176 (2017): 392–401.

81. H. Yang, X. Lan, and Y. Xiong, "Human Lung Epithelial Cells A549 Epithelial-Mesenchymal Transition Induced by PVA/Collagen Nanofiber," *Gels* 8, no. 5 (2022): 279.

82. K. Ngece, B. A. Aderibigbe, D. T. Ndinteh, Y. T. Fonkui, and P. Kumar, "Alginate-Gum Acacia Based Sponges as Potential Wound Dressings for Exuding and Bleeding Wounds," *International Journal of Biological Macromolecules* 172 (2021): 350–359.

83. C. Yu, Y. Lu, and J. Pang, "A Hemostatic Sponge Derived From Chitosan and Hydroxypropylmethylcellulose," *Journal of the Mechanical Behavior of Biomedical Materials* 150 (2024): 106240.

84. M. Li, Z. Z. Zhang, Y. Liang, J. He, and B. Guo, "Multifunctional Tissue-Adhesive Cryogel Wound Dressing for Rapid Nonpressing Surface Hemorrhage and Wound Repair," *ACS Applied Materials & Interfaces* 12 (2020): 35856–35872.

85. F. C. Zanchetta, P. De Wever, J. Morari, et al., "In Vitro and In Vivo Evaluation of Chitosan/HPMC/Insulin Hydrogel for Wound Healing Applications," *Bioengineering (Basel)* 11, no. 2 (2024): 168.

Supporting Information

Additional supporting information can be found online in the Supporting Information section.

10974628, 2025, 39, Downloaded from https://onlinelibrary.wiley.com/doi/10.1002/app.57508 by University Of Witwatersrand, Wiley Online Library on [07/09/2025]. See the Terms and Conditions (https://onlinelibrary.wiley.com/terms-and-conditions) on Wiley Online Library for rules of use; OA articles are governed by the applicable Creative Commons License